Golden Endohedral Main-Group Clusters, [E@Au12]q−: Theoretical Insights Into the 20-e Principle

ARTICLE *in* JOURNAL OF PHYSICAL CHEMISTRY LETTERS · OCTOBER 2013

Impact Factor: 7.46 · DOI: 10.1021/jz401622m

1 AUTHOR:

Alvaro Muñoz-Castro
Universidad Autónoma De Chile
69 PUBLICATIONS **461** CITATIONS

THE JOURNAL OF PHYSICAL CHEMISTRY Letters

Letter

pubs.acs.org/JPCL

Golden Endohedral Main-Group Clusters, $[E@Au_{12}]^{q-}$: Theoretical Insights Into the 20-e Principle

Alvaro Muñoz-Castro*

Departamento de Ciencias Quimicas, Universidad Andres Bello, Republica 275, Santiago 8370146, Chile

Supporting Information

ABSTRACT: The inclusion of a transition metal (M) into an icosahedral Au_{12} cage ($[M@Au_{12}]^q$), was theoretically predicted prior to its experimental characterization on the basis of the jellium model, where the titled system is in accordance with the 18-*ve* principle fulfilling a $1s^21p^61d^{10}$ electronic configuration. In contrast, the inclusion of a p-block element (E) seems not to follow such principle, leading to an open-shell state that in turn exhibits a Jahn−Teller distortion. Hence, the icosahedral structure is no longer the more stable situation. We rationalize the electronic structure of $[E@Au_{12}]$,^{q} denoting the interaction between the endohedral element and the golden cage, which rise to a $1s^21p^62s^21d^{10}$ electronic configuration requiring 20-*ve* as an extension to the 18-*ve* principle. The 20-*ve* count is valid in almost the whole series, with the exception given by E = N, O, F, Cl, and Br.

SECTION: Molecular Structure, Quantum Chemistry, and General Theory

Gold clusters and nanostructures have attracted great interest in the recent years; the development of novel metal clusters with variable sizes has been achieved as an important contribution to several issues such as nanoelectronics, nanosensors, use as building blocks, and biomedicine[1−5] besides their aesthetic structures. Efforts on the understanding of stable gold clusters, coined superatoms, have been devoted to the rationalization of their structural and electronic properties, where numerous theoretical and experimental[6−10] studies have expanded the knowledge in this concern, pursuing the obtention of novel clusters displaying special electronic and structural stability that can be used as seeds for larger clusters.

The chemistry of gold compounds is particularly influenced by the strong relativistic effects,[11−13] leading to unusual structures for gold clusters relative to those for copper and silver, highlighting the tetrahedral Au_{20} cluster[14,15] and the golden fullerene Au_{32} cage cluster.[16] The inclusion of a heteroatom into the gold skeletal structure allows us to the potential tune of the molecular properties, where the influence of a doping atom is of special importance to the field of catalysis.[17] The first endohedral bare gold cluster depicting a high stable closed-shell electronic and geometrical structure, the icosahedral $[W@Au_{12}]$, was predicted using density functional theory (DFT) by Pyykkö and Runeberg[18] on the basis of the 18-electron principle and later confirmed using photoelectron spectroscopy (PES) by Li et al.[19] in conjunction with other isoelectronic heterometallic $[M@Au_{12}]^-$ M = V, Nb, Ta, and $[Re@Au_{12}]^+$ clusters.[20]

Most stable clusters are characterized by particular numbers of valence electrons (*ve*) reflecting the relationship between electronic and structural states, which has been well understood in terms of magic numbers related to a certain numbers of electrons in the valence shells.[21] The jellium shell model,[21−23] allows us to rationalize the electronic structure of clusters where the core electrons and nuclei charge are considered to form a positively uniform background surrounded by "*free*" valence electrons in a set of electronic levels and satisfy the filling order of such model. Usually, the electronic level sequence is defined by $1s^21p^61d^{10}$..., which resembles the orbitals of isolated atoms, where the magic numbers reflect the consecutive closure of these electronic shells (i.e., 2, 8, 18, etc.).[21−23] The $[W@Au_{12}]$ cluster, involves 12 6s electrons from the icosahedral cage and 6 5d electrons from the endohedral atom, fulfilling the 18-*ve* principle,[18] which is also observed for other transition-metal $[M@Au_{12}]^q$ counterparts.[20]

Herein we elucidate the possible inclusion of a main group metal atom enclosed onto the 12-membered icosahedral structure (Figure 1), taking as framework the interaction between atomic shells of the centered metal and the jellium shells derived from the $[Au_{12}]$ cage. Endohedral gold clusters

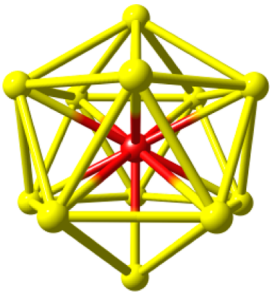

Figure 1. Schematic representation of the icosahedral $[E@Au_{12}]^{q-}$.

Received: July 31, 2013
Accepted: September 22, 2013

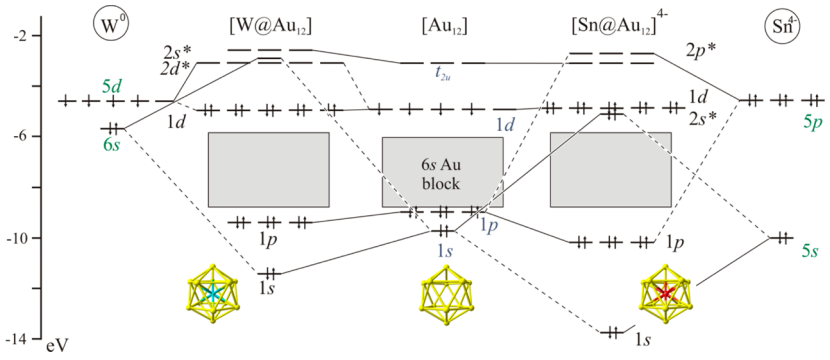

Figure 2. Electronic structure of $[W@Au_{12}]$ (left) and $[Sn@Au_{12}]^{4-}$ (right) denoting the contribution from the central element (W and Sn) and the icosahedral cage ($[Au_{12}]^{0}$). Solid lines denote major contribution to the respective molecular orbital.

involving main-group elements have been characterized for octahedral (Au_6) and trigonal bypiramid (Au_5) phosphine-protected cages.[24] Geometry optimizations and subsequent calculations were performed by using relativistic DFT methods employing the ADF 2012 code[25] with all-electron triple-ξ Slater basis set plus the double-polarization (STO-TZ2P) basis set in conjunction with the nonlocal Perdew–Burke–Ernzerhof (PBE) functional within the generalized gradient approximation (GGA).[26] Relativistic effects were taken into account by ZORA formalism.[27,28] The polarizable continuum model was incorporated into the calculations by considering the conductor-like screening model treatment via the COSMO module[29,30] (dielectric constant ε = 13.5 and rigid-sphere radius = 3.5 Å) to take into account the effects of polar solvent and counterions.

First, we pursue to rationalize the electronic requirements of the endohedral cluster to exhibit a closed-shell configuration evaluating the $Sn@Au_{12}$ system as a case of study. Taking as starting point the 18-*ve* $[W@Au_{12}]$,[18] it is expected that the $Sn@Au_{12}$ cluster also should exhibit a $1s^21p^61d^{10}$ electronic configuration. However, preliminary calculations indicate that the titled cluster in its 18-*ve* form ($[Sn@Au_{12}]^{2-}$; Sn + 12 × Au + q = 4 + 12 + 2 = 18-*ve*) leads to an open-shell electronic configuration that in turn tends to exhibit a Jahn–Teller distortion (i.e., Jahn–Teller effect), varying the structure toward a lesser symmetric and energetic situation,[31,32] in contrast with their stable transition-metal counterparts, 18-*ve* $[M@Au_{12}]^n$. Thus, it is clear that $[Sn@Au_{12}]^{2-}$ does not follow or cannot be interpreted in terms of the 18-*ve* principle.

To achieve a better understanding of the electronic requirements of $Sn@Au_{12}$ cluster, we describe its electronic structure in terms of the interaction diagram between the inner main group element and the jellium levels of the icosahedral structure (Figure 2). The 12 combinations of the 12 6s atomic orbitals of $[Au_{12}]$ under the I_h group span as: $a_g \oplus t_{1u} \oplus h_g \oplus t_{2u}$, which leads to the 1s1p1d and part of the 1f jellium shells,[18,33] which in turn form further bonding/antibonding combinations toward the 5s and 5p shells (a_g and t_{1u}, respectively) of the endohedral Sn atom. This fact gives rise to a new set of jellium states, namely, 1s1p1d2s2p (Figure 3), pointing out the importance of the interaction between the atomic and jellium shells into the generation of the electronic structure of the endohedral cluster. In our case, a 20-*ve* situation ($[Sn@Au_{12}]^{4-}$; 4 + 12 + 4 = 20-*ve*) will fulfill the electronic requirements to achieve a stable icosahedral structure with an $1s^21p^62s^21d^{10}$ electronic configuration, where the two extra electrons in addition to the 18-e principle reside in the

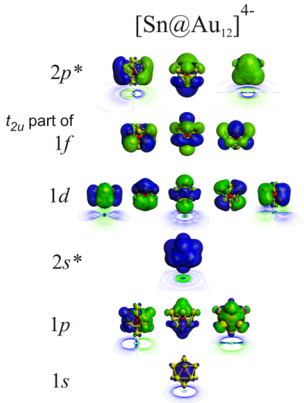

Figure 3. Jellium levels in $[Sn@Au_{12}]^{4-}$, denoting their radial nodes in the contour-plot below.

antibonding combination (2s or 2s*) between the 5s and 1s shells of Sn and $[Au_{12}]$, respectively. It is important to note that the single radial node generated by the nature of such antibonding interaction determines the beginning of the second period or set of jellium levels.

The differences between these 18- and 20-*ve* endohedral clusters, namely, $[W@Au_{12}]$ and $[Sn@Au_{12}]^{4-}$, are ascribed to the interaction between the atomic shells, as can be seen in Figure 2. The formation of $[W@Au_{12}]$ mainly involves the interaction between the s- and d-type shells between the endohedral atom and the inclusive superatom, where the resulting 1s1p1d jellium states remain occupied, as has been described.[18,33] In contrast, the 20-*vec* $[Sn@Au_{12}]^{4-}$ cluster involves the combination between the s- and p-type shells, which leads to a $1s^21p^62s^21d^{10}$ electronic configuration (Figure 3), denoting the antibonding combination between the s-type shells (2s*) located below the 1d shell, resulting in a HOMO–LUMO gap of 1.85 eV with a HOMO eigenvalue of −4.07 eV, close to the obtained for $[W@Au_{12}]$ at the same level of theory (1.87 eV, and HOMO eigenvalue of −5.28 eV). This HOMO–LUMO gap at the B3LYP/ZORA level (2.94 eV, Supporting Information) is in agreement with the initial prediction of $[W@Au_{12}]$, which amounts to 3.0 eV.[19] The estimated interaction energy between the endohedral atom and the gold cage shows that the $[Sn@Au_{12}]^{4-}$ is more favorable than $[W@Au_{12}]$ (−19.70 and −14.10 eV, respectively, including BSSE correction), thus offering a more stable situation to the endohedral structure. This difference in energy reflects that the net p-type interaction in the 20-e cluster is more favorable than the s- and d-type interactions in $[W@Au_{12}]$, as can be

dx.doi.org/10.1021/jz401622m | J. Phys. Chem. Lett. 2013, 4, 3363–3366

concluded from the gap between the respective bonding and antibonding combinations (Figure 2). This fact, in addition to the obtained HOMO−LUMO gap, suggests that the titled 20-*vec* cluster could also be experimentally characterized,[19,20] which is corroborated by using several hybrid, GGA, and *meta*-GGA (Supporting Information, Table S1) functionals denoting similar results. It is important to note that the anionic nature of the $[Sn@Au_{12}]^{4-}$ cluster will consequently require the presence of a polar solvent or counteranions to stabilize the overall charge. These effects were taken into account in our calculations through the inclusion of a polarizable continuum model for the anionic clusters.[29,30]

The present description of the 20-*vec* systems as a 1s1p2s*1d cluster encourages us to extend the current analysis to the whole p-block, retaining the highly symmetrical *icosahedral* structure, which can lead to the obtention of novel clusters or *superatoms*, displaying stable electronic and geometrical structures. In the Supporting Information (Figure S1), we describe the electronic structure of icosahedral $[E@Au_{12}]^{q-}$ clusters concerning the whole p-block denoting each jellium level, namely, for each group, $[E^{XIII}@Au_{12}]^{5-}$, $[E^{XIV}@Au_{12}]^{4-}$, $[E^{XV}@Au_{12}]^{3-}$, $[E^{XVI}@Au_{12}]^{2-}$, and $[E^{XVII}@Au_{12}]^{1-}$. As expected, the 1d and part of the 1f shell t_{2u} are mainly affected by the skeletal Au−Au distances ranging between 2.821 and 3.027 Å, which increase going down a given group (Table S1 in the Supporting Information) and thus remain similar through the series because of the lack of available interacting endohedral orbitals given by symmetry considerations.

The 20-*vec* endohedral cluster displaying an element from the group XIII (E^{XIII} = Al, Ga, In, and Tl) exhibits a 1s1p1d2s*2p* shell order with a $1s^21p^61d^{10}2s^2$* configuration, where a small gap between $1d^{10}$ and $2s^2$* can be observed; this result slightly differs from the above-described shell order of $[Sn@Au_{12}]^{4-}$. For the $[B@Au_{12}]^{5-}$ counterpart and the rest of the elements in the p-block, a $1s^21p^62s^2$*$1d^{10}$ configuration is observed as described for $[Sn@Au_{12}]^{4-}$, where the 1s level of the overall cluster qualitatively decreases the contribution from the 1s from the $[Au_{12}]$ cage (1s-$[Au_{12}]$) toward a more stabilizing situation as the number of the group increases. This overall 1s shell is the most influenced level according to the nature of the endohedral element, denoting a greater stabilization going from group XIII to XVII elements, whereas the 1p, 2s*, and 2p* vary to a small extend. It is important to note that the relative position of the endohedral np function in relation to the jellium levels of the gold-cage in these 20-*ve* clusters determines the electronic configuration in terms of the jellium levels and the behavior of the frontier levels due to the location of the 2p* shell in relation to the 1d shell, which leads to a small HOMO−LUMO gap in some cases, as is observed for E = C, S, Se, I, and At in the range of ∼0.50 eV for C and At and ∼0.25 eV for S, Se, and I (Table S2 in the Supporting Information).

In our search, we found that the systems with E = N, O, F, Cl, and Br in their 20-*ve* form exhibit a level order of 1s1p2s*2p*1d, displaying a $1s^21p^62s^2$*$2p^6$*$1d^4$ configuration with an unfilled 1d shell, thus leading to a Jahn−Teller distortion. This situation is generated because in these systems the 2s* and 2p* shells are located below the 1d shell. (See Figure S1 in the Supporting Information.) Thus, these systems are considered as the exception to the series of p-block 20-*ve* endohedral gold-based cluster.

An interesting example of an icosahedral 20-*ve* cluster in the literature is advised in the multilayer $[Sn@Cu_{12}@Sn_{20}]^{12-}$ intermetalloid,[34] which has been recently formally described as $[\{Sn@Cu_{12}\}^{4-}@\{Sn_{20}\}^{8-}]^{12-}$, where the inner core ($[Sn@Cu_{12}]^{4-}$) denotes a $1s^21p^62s^21d^{10}$ electronic shell configuration (Muñoz-Castro, A., manuscript in preparation), supporting our insights.

In addition, the role of the spin−orbit coupling into the jellium states by using total angular momentum (j) instead of the *pure* orbital angular momentum (l) representations[33,35] is given in the Supporting Information, describing the electronic structure of group XV elements, namely, $[E@Au_{12}]^n$ with E = C, Si, Sn, Ge, and Pb (Figure S1 in the Supporting Information). As has been recently described for $[W@Au_{12}]$,[33] the jellium states with $l \neq 0$ split similarly to the atomic functions, and thus in our case the 20-*vec* configuration can be described as $1s_{1/2}^2\ 1p_{3/2}^4\ 1p_{1/2}^2\ 2s_{1/2}^2\ 1d_{3/2}^4\ 1d_{5/2}^6$.

In conclusion, our study reveals the extension of the 18-*ve* principle in gold-based endohedral clusters, which has been employed to predict the inclusion of transition-metal elements in a $[Au_{12}]$ cage. The 20-*ve* in p-block systems pursues to fulfill a $1s^21p^62s^21d^{10}$ electronic configuration, in contrast with the 18-*ve* where a $1s^21p^61d^{10}$ configuration is achieved. A number of interesting features regarding the electronic structure were characterized, denoting that the main interaction is given between the s- and p-type shells in $[E@Au_{12}]^q$, which leads to bonding and antibonding combinations, which in turn determine the electronic requirements to achieve a stable and highly symmetrical cluster according to a 20-*ve* principle. The location of the 2s* and 2p* shells, which is dependent on the endohedral element in the system in relation to the 1d shell determines the HOMO−LUMO gap in the series and the presence of exceptions observed for E = N, O, F, Cl, and Br. In the series, the endohedral clusters involving the whole group XIII (E^{XIII}), E^{XIV} = Si to Pb, E^{XV} = P to Bi, and E^{XVI} = Po, exhibit HOMO−LUMO gaps larger than 1 eV, which suggest a wide range of doped golden clusters,[36] which should be employed as building blocks or as seeds for larger clusters with promising application as nanomaterials.

In final words, the interaction between the shells of the concentric structures must be taken into account to rationalize the electronic structure of endohedral clusters, which is a useful strategy to design and predict stable homo- and hetero-metallic clusters, highlighting the possibility to obtain doped counterparts. As a consequence, this point is the main difference for the electronic considerations between a hollow and an endohedral cluster.

■ ASSOCIATED CONTENT

Ⓢ Supporting Information

Comparison of the performance of several hybrid, GGA, and meta-GGA functionals into the HOMO−LUMO gap and interaction energy between Sn/W and Au_{12} in $[Sn@Au_{12}]^{4-}$ and $[W@Au_{12}]$; selected geometrical parameters and HOMO−LUMO gaps (H−L gap); electronic structure of $[E@Au_{12}]^{q-}$ denoting the jellium levels; and electronic structure of group XIV $[E@Au_{12}]^{4-}$ denoting the splitting of the levels with $l \neq 0$ due to the spin−orbit coupling term. This material is available free of charge via the Internet at http://pubs.acs.org.

■ AUTHOR INFORMATION

Corresponding Author

*Tel: +56 02 6618249. E-mail alvaro.munoz@unab.cl.

Notes

The authors declare no competing financial interest.

■ ACKNOWLEDGMENTS

The author sincerely thanks the reviewers for their valuable and useful comments. This work has been financially supported by FONDECYT 11100027, UNAB DI-28-12/R, and PROJECT MILLENNIUM No. P07-006-F grants.

■ REFERENCES

(1) *Metal Clusters in Chemistry*; Braunstein, P., Oro, L. A., Raithby, P. R., Eds.; Wiley-VCH: Weinheim, Germany, 1999.
(2) Daniel, M.-C.; Astruc, D. Gold Nanoparticles: Assembly, Supramolecular Chemistry, Quantum-Size-Related Properties, and Applications toward Biology, Catalysis, And Nanotechnology. *Chem. Rev.* **2004**, *104*, 293−346.
(3) Bergeron, D. E.; Castleman, A. W.; Morisato, T.; Khanna, S. N. Formation and Properties of Halogenated Aluminum Clusters. *J. Chem. Phys.* **2004**, *121*, 10456.
(4) Bergeron, D. E.; Roach, P. J.; Castleman, A. W., Jr.; Jones, N. O.; Khanna, S. N. Al Cluster Superatoms as Halogens in Polyhalides and as Alkaline Earths in Iodide Salts. *Science* **2005**, *307*, 231−235.
(5) Homberger, M.; Simon, U. On the Application Potential of Gold Nanoparticles in Nanoelectronics and Biomedicine. *Philos. Trans. R. Soc., A* **2010**, *368*, 1405−1453.
(6) Alonso, J. A. Electronic and Atomic Structure, and Magnetism of Transition-Metal Clusters. *Chem. Rev.* **2000**, *100*, 637−677.
(7) Häkkinen, H. Atomic and electronic structure of gold clusters: understanding flakes, cages and superatoms from simple concepts. *Chem. Soc. Rev.* **2008**, *37*, 1847−1859.
(8) Jena, P. Beyond the Periodic Table of Elements: The Role of Superatoms. *J. Phys. Chem. Lett.* **2013**, *4*, 1432−1442.
(9) Zhu, M.; Aikens, C. M.; Hollander, F. J.; Schatz, G. C.; Jin, R. Correlating the Crystal Structure of A Thiol-Protected Au25 Cluster and Optical Properties. *J. Am. Chem. Soc.* **2008**, *130*, 5883−5885.
(10) *Cluster and Nano-Assemblies*; Jena, P., Khanna, S. N., Rao, B. K., Eds.; World Scientific: Singapore, 2003.
(11) Pyykkö, P. Relativistic Effects in Structural Chemistry. *Chem. Rev.* **1988**, *88*, 563−594.
(12) Schwerdtfeger, P. Relativistic Effects in Properties of Gold. *Heteroat. Chem.* **2002**, *13*, 578−584.
(13) Schmidbaur, H.; Schier, A. Aurophilic Interactions As a Subject of Current Research: An Up-Date. *Chem. Soc. Rev.* **2012**, *41*, 370−412.
(14) Li, J.; Li, X.; Zhai, H.-J.; Wang, L.-S. Au_{20}: A Tetrahedral Cluster. *Science* **2003**, *7* (299), 864−867.
(15) Zhang, H.-F.; Stender, M.; Zhang, R.; Wang, C.; Li, J.; Wang, L.-S. Toward the Solution Synthesis of the Tetrahedral Au_{20} Cluster. *J. Phys. Chem. B* **2004**, *108*, 12259−12628.
(16) Johansson, M. P.; Sundholm, D.; Vaara, J. Au_{32}: A 24-Carat Golden Fullerene. *Angew. Chem., Int. Ed.* **2004**, *43*, 2678−2681.
(17) Häkkinen, H.; Abbet, S.; Sanchez, A.; Heiz, U.; Landman, U. Structural, Electronic, And Impurity-Doping Effects in Nanoscale Chemistry: Supported Gold Nanoclusters. *Angew. Chem., Int. Ed.* **2003**, *42*, 1297−1300.
(18) Pyykkö, P.; Runeberg, N. Icosahedral WAu_{12}: A Predicted Closed-Shell Species, Stabilized by Aurophilic Attraction and Relativity and in Accord with the 18-Electron Rule. *Angew. Chem., Int. Ed.* **2002**, *41*, 2174−2176.
(19) Li, X.; Kiran, B.; Li, J.; Zhai, H.-J..; Wang, L.-S. Experimental Observation and Confirmation of Icosahedral $W@Au_{12}$ and $Mo@Au_{12}$ Molecules. *Angew. Chem., Int. Ed.* **2002**, *41*, 4786−4789.
(20) Zhai, H.-J.; Li, J.; Wang, L.-S. Icosahedral Gold Cage Clusters: MAu_{12}− (M=V, Nb, and Ta). *J. Chem. Phys.* **2004**, *121*, 8369.
(21) Knight, W. D.; Clemenger, K.; de Heer, W. A.; Saunders, W. A.; Chou, M. Y.; Cohen, M. L. Electronic Shell Structure and Abundances of Sodium Clusters. *Phys. Rev. Lett.* **1984**, *52*, 2141−2143.
(22) De Heer, W. A. The Physics of Simple Metal Clusters: Experimental Aspects and Simple Models. *Rev. Mod. Phys.* **1993**, *65*, 611−676.
(23) Lin, Z.; Slee, T.; Mingos, D. M. P. a Structural Jellium Model of Cluster Electronic Structures. *Chem. Phys.* **1990**, *142*, 321−334.
(24) Häberlen, O. D.; Schmidbauer, H.; Rösch, N. Stability of Main-Group Element-Centered Gold Cluster Cations. *J. Am. Chem. Soc.* **1994**, *116*, 8241−8248.
(25) *Amsterdam Density Functional (ADF) Code*, release 2012; Vrije Universiteit: Amsterdam, The Netherlands, 2012. http://www.scm.com.
(26) Perdew, J. P.; Burke, K.; Ernzerhof, M. Generalized Gradient Approximation Made Simple. *Phys. Rev. Lett.* **1996**, *77*, 3865−3868.
(27) van Lenthe, E.; Baerends, E. J.; Snijders, J. G. Relativistic Total Energy Using Regular Approximations. *J. Chem. Phys.* **1994**, *101*, 9783.
(28) Dyall, K. G. Fægri, K. *Introduction to Relativistic Quantum Chemistry*; Oxford University Press: New York, 2007 and references therein.
(29) Klamt, A.; Jonas, V. Treatment of Outlying Charge in Continuum Solvation Models. *J. Chem. Phys.* **1996**, *105*, 9972−9980.
(30) Klamt, A. Conductor-like Screening Model for Real Solvents: A New Approach to the Quantitative Calculation of Solvation Phenomena. *J. Chem. Phys.* **1995**, *99*, 2224−2235.
(31) Jahn, H. A.; Teller, E. Stability of Polyatomic Molecules in Degenerate Electronic States. I. Orbital Degeneracy. *Proc. R. Soc. London, Ser. A* **1937**, *161*, 220−235.
(32) Arratia-Perez, R.; Ramos, A. F.; Malli, G. L. Calculated Electronic Structure of Au_{13} Clusters. *Phys. Rev. B* **1989**, *39*, 3005−3009.
(33) Muñoz-Castro, A.; Arratia-Perez, R. Spin-Orbit Effects on a Gold-Based Superatom: A Relativistic Jellium Model. *Phys. Chem. Chem. Phys.* **2012**, *14*, 1408−1411.
(34) Stegmaier, S.; Fässler, T. F. A Bronze Matryoshka: The Discrete Intermetalloid Cluster $(Sn@Cu_{12}@Sn_{20})^{12-}$ in the Ternary Phases $A_{12}Cu_{12}Sn_{21}$ (A = Na, K). *J. Am. Chem. Soc.* **2011**, *133*, 19758−19768.
(35) Muñoz-Castro, A.; Mac-Leod Carey, D.; Arratia-Perez, R. Inside a Superatom: The M_7^q (M = Cu, Ag, q = 1^+, 0, 1^-) Case. *ChemPhysChem* **2010**, *11*, 646−650.
(36) Schwerdtfeger, P. Gold Goes Nano-From Small Clusters to Low-Dimensional Assemblies. *Angew. Chem., Int. Ed.* **2003**, *42*, 1892−1895.